



PUBLISHED FOR SISSA BY SPRINGER

RECEIVED: January 20, 2016

ACCEPTED: March 1, 2016

PUBLISHED: March 14, 2016

# The light bound states of supersymmetric SU(2) Yang-Mills theory

Georg Bergner,<sup>a</sup> Pietro Giudice,<sup>b</sup> Gernot Münster,<sup>b</sup> Istvan Montvay<sup>c</sup>  
and Stefano Piemonte<sup>d</sup>

<sup>a</sup>Albert Einstein Center for Fundamental Physics,  
Institute for Theoretical Physics, University of Bern,  
Sidlerstr. 5, CH-3012 Bern, Switzerland

<sup>b</sup>University of Münster, Institute for Theoretical Physics,  
Wilhelm-Klemm-Str. 9, D-48149 Münster, Germany

<sup>c</sup>Deutsches Elektronen-Synchrotron DESY,  
Notkestr. 85, D-22603 Hamburg, Germany

<sup>d</sup>University of Regensburg, Institute for Theoretical Physics,  
Universitätsstr. 31, D-93040 Regensburg, Germany

E-mail: [montvay@mail.desy.de](mailto:montvay@mail.desy.de), [bergner@itp.unibe.ch](mailto:bergner@itp.unibe.ch),  
[p.giudice@uni-muenster.de](mailto:p.giudice@uni-muenster.de), [munsteg@uni-muenster.de](mailto:munsteg@uni-muenster.de),  
[stefano.piemonte@ur.de](mailto:stefano.piemonte@ur.de)

**ABSTRACT:** Supersymmetry provides a well-established theoretical framework for extensions of the standard model of particle physics and the general understanding of quantum field theories. We summarise here our investigations of  $\mathcal{N} = 1$  supersymmetric Yang-Mills theory with SU(2) gauge symmetry using the non-perturbative first-principles method of numerical lattice simulations. The strong interactions of gluons and their superpartners, the gluinos, lead to confinement, and a spectrum of bound states including glueballs, mesons, and gluino-glueballs emerges at low energies. For unbroken supersymmetry these particles have to be arranged in supermultiplets of equal masses. In lattice simulations supersymmetry can only be recovered in the continuum limit since it is explicitly broken by the discretisation. We present the first continuum extrapolation of the mass spectrum of supersymmetric Yang-Mills theory. The results are consistent with the formation of supermultiplets and the absence of non-perturbative sources of supersymmetry breaking. Our investigations also indicate that numerical lattice simulations can be applied to non-trivial supersymmetric theories.

**KEYWORDS:** Lattice Quantum Field Theory, Supersymmetric gauge theory

ARXIV EPRINT: [1512.07014](https://arxiv.org/abs/1512.07014)

---

**Contents**

<b>1</b>	<b>Introduction</b>	<b>1</b>
<b>2</b>	<b><math>\mathcal{N} = 1</math> supersymmetric Yang-Mills theory</b>	<b>3</b>
<b>3</b>	<b>Numerical lattice simulations</b>	<b>4</b>
3.1	Lattice formulations and simulation methods	4
3.2	Simulation parameters	5
3.3	Particle operators on the lattice	6
3.4	Supersymmetric Ward identities	6
<b>4</b>	<b>New results at <math>\beta = 1.9</math></b>	<b>7</b>
<b>5</b>	<b>Extrapolations to the continuum limit</b>	<b>8</b>
5.1	Low-lying masses	8
5.2	Glueballs	9
5.3	Comparison between $r_0$ and $w_0$	10
<b>6</b>	<b>Improved lattice formulations</b>	<b>11</b>
<b>7</b>	<b>Conclusions</b>	<b>12</b>
<b>A</b>	<b>Tables</b>	<b>14</b>

---

**1 Introduction**

$\mathcal{N} = 1$  supersymmetric Yang-Mills theory (SYM) is the supersymmetric extension of the gluonic sector of the Standard Model. It contains non-Abelian gauge fields of an  $SU(N)$  gauge group interacting with their fermionic superpartners, the gluino fields. Different from the quarks of QCD, the gluinos are Majorana fermions and they transform according to the adjoint representation of the gauge group. The complexity of SYM is comparable to QCD. Several basic properties, like asymptotic freedom, are shared among these two theories [1]. At low temperatures SYM is assumed to confine the gluons and gluinos into colourless bound states, similarly to the mesons and glueballs in QCD. Like in QCD, the investigation of the bound states is a non-perturbative problem that can be addressed by numerical lattice simulations.

Supersymmetry (SUSY) is the essential feature distinguishing SYM from QCD. If SUSY is unbroken, the bound states are arranged in supermultiplets, containing bosonic and fermionic particles with equal masses. The key aspect of the investigations of SYM is to verify the formation of these multiplets. The obtained mass spectrum provides insights

into the low energy effective action of SYM. Effective actions have been constructed in [2] and extended in [3, 4]. Later the question about the existence of SUSY breaking vacua has been raised in [5], which would imply a completely different mass spectrum. Another interesting aspect is the existence of a stable light scalar in the theory, since in addition to the fermion, the multiplet always contains a scalar and a pseudoscalar particle. In SYM the scalar is therefore a natural component of the effective theory, whereas the interpretation of its QCD counterpart is more controversial [6]. A light scalar state is also essential for technicolour and composite Higgs theories. The predicted degeneracy of the multiplet masses provides a test of our methods for the challenging measurements of this state.

An important characteristic of SUSY is the non-trivial interplay with the space-time symmetries. For example, the anticommutator of the SUSY generators  $Q_\alpha$  is connected with the generators of translations  $P_\mu$ :

$$\{Q_\alpha, Q_\beta\} = (C\gamma_\mu)_{\alpha\beta}P_\mu. \quad (1.1)$$

The absence of the infinitesimal translations generated by  $P_\mu$  is an illustration of the unavoidable SUSY breaking on the lattice. In a more detailed analysis one can prove that supersymmetry is generically broken on the lattice [7]. In most cases there is no restoration of SUSY in the continuum limit without a fine tuning of certain SUSY breaking counterterms. In SYM it is the fine tuning of the bare gluino mass. Our simulations are an important test for the general applicability of non-perturbative lattice methods for SUSY theories. It is one of the few non-trivial four-dimensional examples where the complete restoration of SUSY in the continuum limit can be shown in terms of the Ward identities and the degenerate mass spectrum.

The main focus of our investigations is the spectrum of bosonic and fermionic bound states. In addition we have investigated the supersymmetric Ward identities, static potential, thermal behaviour and other quantities. Compared to QCD, the determination of the masses of meson-like bound states in SYM is significantly more demanding, because all mesons are flavour singlets and the calculation of their correlators requires the notoriously difficult disconnected contributions. Like their QCD counterparts, the glueball operators require a large statistics for a reasonable signal.

This article concludes our studies of the bound states spectrum of SU(2) SYM, see [8–12] and references therein for previous work of our collaboration. In [8] a rather large gap between bosonic and fermionic masses in the mass spectrum was obtained. In later investigations [12] we have found that this effect significantly decreases at a smaller lattice spacing. In this article we present the results at a third, even smaller, lattice spacing, which allow an extrapolation to the continuum limit.

In section 2 we will give a short overview of the SYM in the continuum. We describe the numerical setup for the lattice action and the analysis in section 3. Section 4 summarises our new data at our smallest reliable lattice spacing. In combination with our previous results the new data allow the continuum extrapolation of the spectrum as presented in section 5. Based on this extrapolation, in section 6 we estimate the effects of improvements of the lattice action that are an interesting starting point for future investigations of the theory.

## 2 $\mathcal{N} = 1$ supersymmetric Yang-Mills theory

SYM has one conserved supercharge that transforms bosonic and fermionic states into each other. In particular the gluino, a spin-1/2 Majorana fermion in the adjoint representation of the gauge group  $SU(N)$ , is the superpartner of the gluon.

SYM shows confinement at low energies and the gluons and gluinos form bound states. In that respect it is similar to QCD, where the hadrons are formed of the elementary quarks and gluons. On the other hand, SYM represents the pure gluonic part of supersymmetric QCD and leads to the confinement of external fundamental charges, corresponding to heavy fundamental quarks. The linear rise of the static quark potential with a non-zero string tension  $\sigma$  is a measurable signal of this effect. Since the fermions are in the adjoint representation, string breaking does not occur at any distance, like in pure Yang-Mills theory. A deconfinement phase transition is expected at a critical temperature  $T_c$  that separates this low energy regime from the gluino-gluon plasma at high temperature. First results have been presented in [13], where a second order phase transition has been observed at a temperature  $T_c \simeq 200$  MeV in QCD units.

In the continuum the off-shell Lagrangian of SYM reads

$$\mathcal{L} = -\frac{1}{4}\text{Tr}(F_{\mu\nu}F^{\mu\nu}) + \frac{i}{2}\bar{\lambda}(x)\gamma^\mu D_\mu\lambda(x) + D^a(x)D_a(x), \quad (2.1)$$

where  $D_\mu$  denotes the covariant derivative in the adjoint representation. The auxiliary field  $D^a(x)$ , needed to ensure supersymmetry off-shell, has no kinetic term and can be integrated out from the partition function. After adding a gluino mass term, that breaks SUSY softly, the resulting on-shell Lagrangian is thus given by

$$\mathcal{L} = -\frac{1}{4}\text{Tr}(F_{\mu\nu}F^{\mu\nu}) + \frac{i}{2}\bar{\lambda}(x)\gamma^\mu D_\mu\lambda(x) - \frac{m_g}{2}\bar{\lambda}\lambda. \quad (2.2)$$

In one-flavour QCD the action would look quite similar and the chiral symmetry would correspond to  $U(1)_A \times U(1)_V$  with a  $U(1)_A$  broken by the anomaly and the unbroken  $U(1)_V$ , which corresponds to the conserved baryon number. In SYM the action is invariant under a  $U(1)_R$  chiral symmetry that is broken down to  $Z_N$  by the anomaly. The formation of the gluino condensate leads to an additional spontaneous breaking down to  $Z_2$ . The remaining symmetry corresponds to the fermion number conservation modulo 2 for Majorana fermions.

Based on low-energy effective actions, predictions have been made for two low-lying chiral supermultiplets [2–4]. One of them contains a scalar meson  $a-f_0$ , represented by the interpolating field  $\bar{\lambda}\lambda$ , a pseudo-scalar meson  $a-\eta'$ , represented by  $\bar{\lambda}\gamma_5\lambda$ , and a gluino-gluon state. The gluino-gluon is an exotic particle, which does not have a counterpart in QCD. It is a spin 1/2 Majorana fermion, which can be created by the operator

$$\tilde{O}_{g\tilde{g}} = \sum_{\mu\nu} \sigma_{\mu\nu} \text{Tr} [F^{\mu\nu}\lambda], \quad (2.3)$$

with  $\sigma_{\mu\nu} = \frac{1}{2}[\gamma_\mu, \gamma_\nu]$ . The other supermultiplet consists of a scalar  $0^{++}$  glueball, a pseudoscalar  $0^{-+}$  glueball, and a gluino-gluon particle.

### 3 Numerical lattice simulations

#### 3.1 Lattice formulations and simulation methods

A lattice action for the Euclidean version of SYM has been proposed by Curci and Veneziano [14]. The action for the gauge fields is the usual Wilson action, which in our calculations has been extended to the tree-level Symanzik improved gauge action. The gluinos are described by Wilson fermions in the adjoint representation. In our case stout smearing [15] is applied on the gauge links in the Wilson-Dirac operator.

The Curci-Veneziano action explicitly breaks supersymmetry and the  $U(1)_R$  symmetry. To recover the continuum symmetries the necessary fine-tuning of supersymmetry and  $U(1)_R$  symmetry can be achieved through the same parameter, namely the bare gluino mass represented by the fermionic hopping parameter  $\kappa$  [14, 16]. To approach the limit of a vanishing gluino mass, the bare parameter  $\kappa$  has to be tuned to the critical value  $\kappa_c$  that corresponds to the point where all explicit chiral symmetry breaking terms vanish in the continuum limit. The value of  $\kappa_c$  is most easily obtained from the dependence of the adjoint pion ( $a-\pi$ ) mass on  $\kappa$ . The correlator of this particle is the connected contribution of the  $a-\eta'$  correlator. Even though  $a-\pi$  is not a physical state of SYM, it can be defined in a partially quenched setup where the chiral limit is identified with the point where the adjoint pion mass vanishes [17].

The updates of gauge configurations are performed with the two-step polynomial hybrid Monte Carlo (PHMC) algorithm [8, 18]. The polynomial approximation is less precise for small eigenvalues of the Hermitian Wilson-Dirac operator that can appear in the simulations for  $\kappa$  close to  $\kappa_c$ . When necessary, this error is corrected by a reweighting with correction factors in the analysis. These are obtained from the exact contribution of the lowest eigenvalues.

Our lattice formulation leads to a mild sign problem, arising as  $O(a)$  lattice artefact. The Pfaffian obtained from the integration of the Majorana fermions can sometimes have a negative sign [19], especially close to the chiral limit. This sign is included in the reweighting, if necessary. To reduce the statistical errors we have chosen the parameters of our present simulations such that the reweighting with correction factors and Pfaffian signs is not significant for the final results. In general the relevance of the reweighting is reduced at the smaller lattice spacings and for higher levels of stout smearing.

In principle it is also possible to formulate the model using Ginsparg-Wilson type fermions. In such a formulation the parameter values, at which the chiral and supersymmetric continuum limit is to be found, are known and thus do not need fine tuning. Also, this formulation does not have a sign problem of the Pfaffian. Supersymmetry breaking at non-zero lattice spacings is, of course, still unavoidable. Interesting results have been obtained in some studies of the chiral condensate using this type of lattice formulation [20–22]. The determination of the mass spectrum requires, however, rather large lattices, which leads to a high computational cost with these formulations. We have found in our studies that the fine-tuning is feasible without problems, and hence there is no particular need for the use of Ginsparg-Wilson type formulations in our investigations.

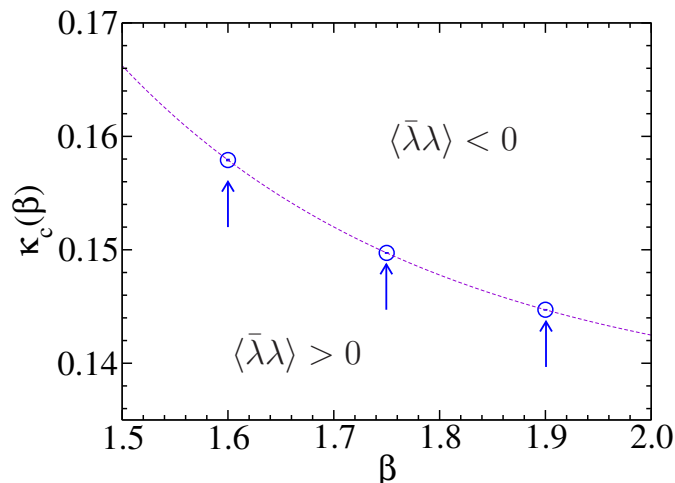


**Figure 1.** Masses of particles are first extrapolated to the chiral limit, i. e. to the critical value of  $\kappa$  where the gluino mass vanishes, and then to the continuum limit,  $\beta \rightarrow \infty$ . The critical line  $\kappa_c(\beta)$  separates the bare parameter space into two regions characterised by either a positive or a negative expectation value of the gluino condensate. Chiral extrapolations at  $\beta = 1.6$  and  $\beta = 1.75$  have been presented in ref. [8] and refs. [10, 12], respectively.

### 3.2 Simulation parameters

We have chosen the lattice sizes such that finite volume effects can be neglected in comparison with statistical errors, based on our investigation in [10]. Since lattice artifacts are the most relevant systematic errors, the most reliable results would be obtained at the smallest lattice spacings. The lattice spacing can, however, not be easily reduced to arbitrary small values since topology freezing introduces very large autocorrelation times and uncertainties in the observables at a small lattice spacing [23]. This problem can be reduced by choosing longer HMC trajectories in the gauge field update, for instance trajectories of length 2, which we had in most of our simulations at larger  $\beta$  values. In spite of that we have found a significant influence of topology freezing at  $\beta = 2.1$ , where the lattice spacing in QCD units (where the Sommer parameter  $r_0$  is set to 0.5 fm) would be around 0.02 fm. For instance, at  $\beta = 2.1$ ,  $\kappa = 0.1397$  on a  $48^3 \cdot 96$  lattice we observe for the topological charge  $Q$  an integrated autocorrelation time  $\tau_Q \simeq 145$ , whereas at  $\beta = 1.9$ ,  $\kappa = 0.14415$  on a  $32^3 \cdot 64$  lattice we have  $\tau_Q \simeq 24$ . In addition to the longer autocorrelation, at  $\beta = 2.1$  it is very difficult to achieve a distribution of  $Q$  symmetric about 0. Topology freezing represents an upper limit for the parameter  $\beta$  in the simulations unless open boundary conditions are introduced or the statistic is increased by about an order of magnitude.

In this work we present our new results of simulations at  $\beta = 1.9$  which are summarised in table 1 and discussed in more detail in section 4. Including our previous simulations, three different values of the inverse gauge coupling  $\beta$ , corresponding to three lattice spacings  $a$  have been considered. For each  $\beta$ , several values of the fermionic hopping parameter  $\kappa$  have been chosen in order to extrapolate to  $\kappa_c$ , see figure 1. The parameters of the simulations at the two larger lattice spacings at  $\beta = 1.6$  and 1.75 have been presented in previous publications [8, 10, 12].

### 3.3 Particle operators on the lattice

The mesonic operators are similar to the flavour singlet meson operators in QCD. The scalar meson corresponds to the adjoint version of  $f_0$  ( $a\text{-}f_0$ ), and the pseudoscalar to the adjoint  $\eta'$  meson ( $a\text{-}\eta'$ ). The correlators for these particles are a sum of disconnected and connected fermion contributions. In QCD the connected part corresponds to the pion, while in SYM an adjoint pion ( $a\text{-}\pi$ ) is not a physical state of the theory, but can be defined in a partially quenched setup [17]. It provides the best signal to noise ratio of all the considered states and the most reliable basis for determining the critical value  $\kappa_c$  of the hopping parameter where the gluino mass vanishes.

The determination of the disconnected contributions is rather challenging. They are determined by a stochastic estimation combined with the exact contribution of the lowest eigenvalues of the Hermitian Dirac-Wilson operator and truncated solver techniques to reduce the fluctuations of the signal. Similar to QCD, the disconnected contributions yield the most relevant uncertainty in the mesonic operators.

The gluino-gluon is measured with a lattice version of the operator of eq. (2.3), where the  $F_{\mu\nu}$  part is replaced by the clover plaquette. APE and Jacobi smearing is applied to get a better signal for the ground state [10].

The glueball masses are determined on the lattice by operators based on the product of link variables. In our study the interpolating operator for the scalar glueball  $0^{++}$  is given by the fundamental plaquette built from four links, while for the glueball  $0^{-+}$  it is given by the product of eight links with suitable shape [24].

In order to reduce the contamination from excited states and therefore determine the effective mass already at small time-slice separation we used the variational method based on APE smeared operators [25]. In total between  $L = 16$  and  $L = 18$  different operators were used in the variational method, each separated by  $N_{APE}$  steps. The smearing parameter was usually fixed to  $\epsilon_{APE} = 0.5$ , while  $N_{APE} = 4$  for the volume  $24^3$  and  $N_{APE} = 5$  for the volume  $32^3$ . As in QCD, the glueballs are characterised by a small signal-to-noise ratio compared to the other observables.

### 3.4 Supersymmetric Ward identities

An important issue in our approach is the determination of the point in parameter space where the theory is characterised by a massless gluino. In this point not only the explicit chiral symmetry breaking by the gluino mass disappears, but also, in the continuum limit, SUSY is restored.

A renormalised gluino mass can be defined on the lattice by means of the supersymmetric Ward identities (SWI) [26]. They give the (subtracted) gluino mass up to a renormalisation factor ( $am_S Z_S^{-1}$ ).

On the other hand, the point of vanishing gluino mass can be estimated in an indirect way from the vanishing of the adjoint pion mass. The adjoint-pion mass squared  $a\text{-}\pi$  is expected to vanish linearly with the (renormalised) gluino mass  $m_{a\text{-}\pi}^2 \propto m_g$ . This relation was obtained in the OZI approximation in [2], and derived in [17] in a partially quenched setup.

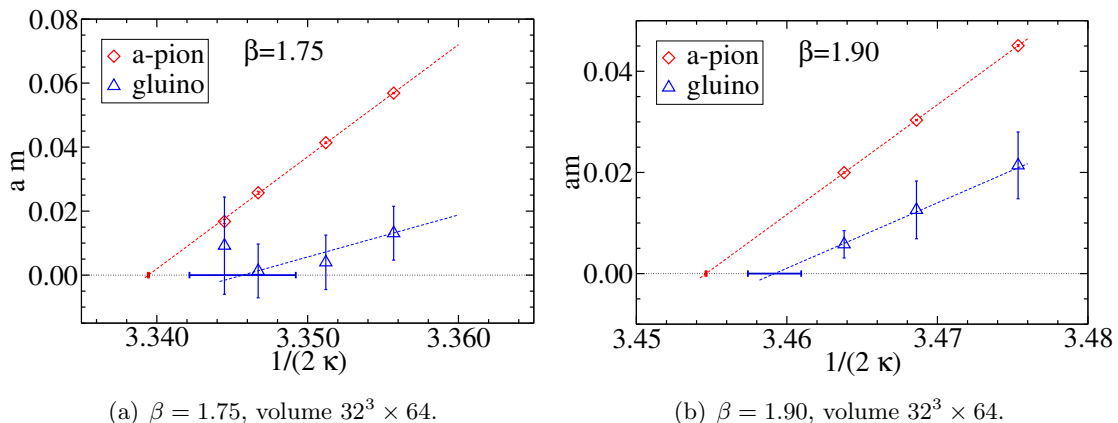


**Figure 2.** Comparison between the values of  $\kappa_c$  defined as the value of  $\kappa$  where the square of the a- $\pi$  mass (a-pion) or the renormalised gluino mass  $am_S Z_S^{-1}$  (gluino) vanishes. The horizontal thick lines (red and blue) show the uncertainty in the determination of the intercept with zero.

The parameter which we tune to get a zero gluino mass is  $\kappa$ . In general, the a- $\pi$  mass yields a more precise determination of  $\kappa_c$ . In principle, different definition of the renormalised gluino mass will agree up to  $O(a)$  lattice artefacts. In previous studies we have checked that both signals lead within our statistical errors to a consistent value of  $\kappa_c$  [8].

We have measured the SWI in our new set of configurations, closest to the continuum limit, at  $\beta = 1.75$  and at  $\beta = 1.9$ , to check again the agreement in the determination of  $\kappa_c$ . In figure 2 we plot the value of  $am_S Z_S^{-1}$  (labelled as gluino) and the square of the adjoint pion mass (labelled as a-pion).

We can see that the two values are compatible within two standard deviations both at  $\beta = 1.75$  and  $\beta = 1.9$ . Taking into account that the determination of  $am_S Z_S^{-1}$  is a complex procedure, it is difficult to estimate its systematic errors, and we consider both determinations to be acceptable and the two methods to be compatible.

Because the value of  $\kappa_c$  determined via a- $\pi$  is by far more precise, the tuning of  $\kappa$  is done using this quantity.

#### 4 New results at $\beta = 1.9$

To estimate the masses of the bound states in the continuum at zero gluino mass a two-fold extrapolation has to be made. In the first step, at each fixed value of  $\beta$  the masses are extrapolated in  $\kappa$  to the limit of a vanishing gluino mass at  $\kappa_c$ . As explained above, the masses as a function of the squared mass of the adjoint pion ( $m_{a-\pi}$ ) are extrapolated to the “chiral limit”  $m_{a-\pi} = 0$ . We consider a mass independent scale setting scheme, in which the lattice spacing is constant at fixed  $\beta$ . Therefore the extrapolations to the chiral limit can be done directly for the masses in lattice units ( $am$ ).

The masses in lattice units, obtained from our simulations at  $\beta = 1.9$ , are presented in table 1. Figure 3 shows the extrapolation of the masses to the chiral limit. As for the  $\beta = 1.75$  case, the spectrum is almost degenerate in the chiral limit, which is quite different from our previous results at  $\beta = 1.6$ . This qualitative observation can now be made more rigorous by a complete extrapolation to the continuum limit.



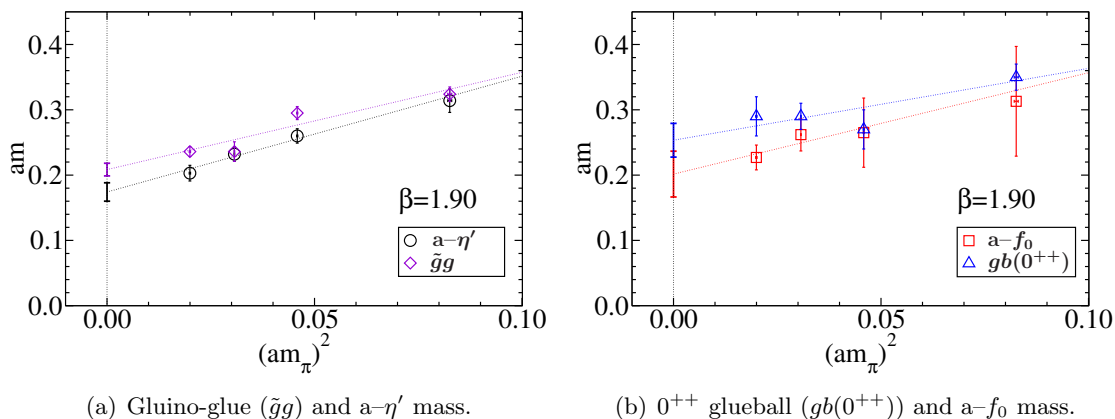


**Figure 3.** Extrapolation to the chiral limit ( $m_{a-\pi} = 0$ ) at  $\beta = 1.90$ .

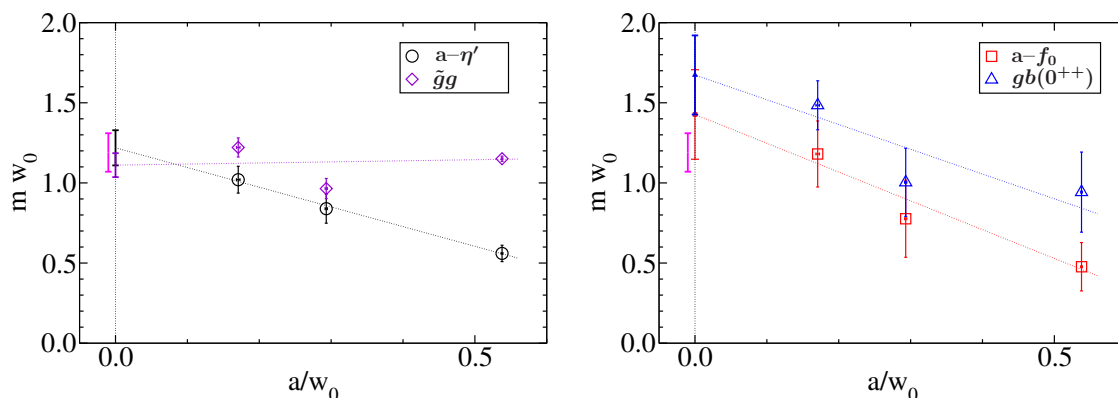
## 5 Extrapolations to the continuum limit

### 5.1 Low-lying masses

The first extensive studies of our collaboration at the lattice spacing  $a$  corresponding to  $\beta = 1.6$  have found a mass of the gluino-gluon particle ( $m_{\tilde{g}g}$ ) that was significantly heavier than the masses of the other particles of the expected multiplet [8]. In a second step  $a$  has been reduced, corresponding to a larger value of  $\beta = 1.75$ , and a significant reduction of the gap between  $m_{\tilde{g}g}$  and  $m_{a-\eta'}$  has been observed [10, 12]. The new results at the third smaller lattice spacing at  $\beta = 1.9$  now allow to present the first extrapolation to the continuum limit of the lowest bound state masses. The large mass splitting between the bosonic bound states and their fermionic counterpart that was visible at  $\beta = 1.6$  has been significantly reduced at the smaller lattice spacings.

Results at different lattice spacings  $a$  can be combined in an extrapolation to the continuum limit ( $a \rightarrow 0$ ) once an observable is chosen to set the scale, i. e. to define the physical length associated with  $a$ . The scale setting is a large source of systematic errors, therefore several different observables have been computed for the extrapolation to the continuum limit. The determination of the scale for our model has been presented in ref. [27]. To extrapolate to the continuum limit, we have chosen the Wilson flow quantity  $w_0$  defined at the reference time  $\tau = 0.3$ . The lattice spacing is implicitly defined by the obtained numerical value of the dimensionless quantity  $a/w_0$ . The Sommer parameter  $r_0$  could be a valid alternative, it has, however, more systematic uncertainties than  $w_0$ , since it requires complex fitting procedures of the noisy expectation values of Wilson loops. The corresponding results are listed in table 3 for the three values of  $\beta$ . Our current method for setting the scale is different from our previous studies, where  $r_0$  has been chosen to set the scale.

All chiral extrapolations have now been redone based on bare quantities in lattice units as in section 4. The error of the scale setting does hence not propagate into the chiral extrapolations, which leads to smaller errors. At  $\beta = 1.75$  we have now split the chiral fit into the ensembles with one and three levels of stout smearing, even though the results



(a) Gluino-gluon ( $\tilde{g}g$ ) and  $a-\eta'$  mass. (b)  $0^{++}$  glueball ( $gb(0^{++})$ ) and  $a-f_0$  mass.

**Figure 4.** (a) Extrapolations of the  $a-\eta'$  and gluino-gluon masses to the continuum limit. The large gap visible at the largest lattice spacing is drastically reduced at larger  $\beta$ . (b) Extrapolations of the  $a-f_0$  and  $0^{++}$  glueball masses to the continuum limit. The extrapolation of the glueball mass is unstable and dominated by the result at small lattice spacing, therefore the final result is compatible with the gluino-gluon mass only within two standard deviations. The thick vertical magenta line represents the weighted mean value of the four masses.

are compatible within errors. In this way the complete extrapolation is now based only on data obtained with one level of stout smearing.

We have also redetermined the glueball masses  $\beta = 1.6$  with a more accurate variational analysis. This leads to a reduced difference between the gluino-gluon and the glueball compared to our previous publication [8].

The extrapolations of the masses to the continuum, using  $w_0$  for the scale setting, are displayed in figures 4(a) and 4(b).

Using  $w_0$  to set scale, the final extrapolation to the continuum limit can be read in table 4, labelled as  $s = w_0$ :

$$w_0 m_{a-\eta'} = 1.22(11) \tag{5.1}$$

$$w_0 m_{a-f_0} = 1.43(28) \tag{5.2}$$

$$w_0 m_{\tilde{g}g} = 1.111(74) \tag{5.3}$$

$$w_0 m_{\text{glueball } 0^{++}} = 1.67(25). \tag{5.4}$$

The masses of  $a-\eta'$ ,  $a-f_0$  and  $\tilde{g}g$  are compatible with the weighted mean value  $w_0 \bar{m} = 1.19(12)$  of the four masses within one standard deviation, while the mass of the  $0^{++}$  glueball is compatible with it by only two standard deviations. However, the glueball has the worst signal-to-noise ratio and the extrapolation of its mass to the continuum limit is less reliable due to the large errors at fine lattice spacing.

## 5.2 Glueballs

The picture of a lower supermultiplet consisting of bound states of gluons and a higher one of mesons was proposed in [4]. On the other hand, in [28] the authors, using different

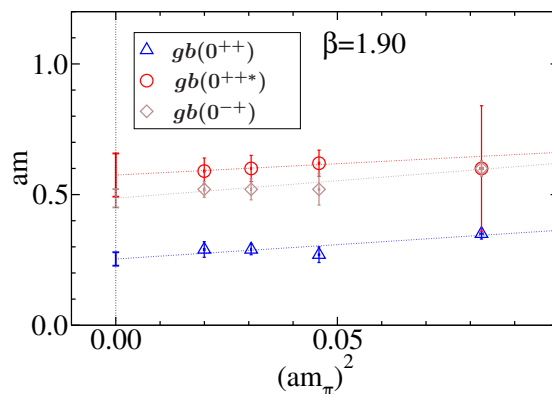


**Figure 5.** Glueball spectrum at  $\beta = 1.9$ . The mass of the first excited state of the  $0^{++*}$  glueball, which is twice the mass of the  $0^{++}$  glueball ground state, appears to be compatible with the fundamental mass of the  $0^{-+}$  glueball.

arguments and experience from QCD, deduce the opposite ordering of multiplets. The  $0^{++}$  glueball and the gluinoball  $a-f_0$  on the one hand, and the  $0^{-+}$  glueball and the gluinoball  $a-\eta'$  on the other hand have the same quantum numbers, and they might be characterised by a strong mixing. In that case it would be difficult to say which of the two supermultiplets is more glueball-like or gluino-like, since we will get the same mass from both of them, namely the one of the lightest state. This is the case shown in figure 4(b), where  $0^{++}$  and  $a-f_0$  have compatible masses.

On the other hand, if the mixing of the states is weak, it is possible that the two operators project onto two different states, and two different masses are obtained in this case. Our results seem to suggest that the  $0^{-+}$  glueball and the  $a-\eta'$  have a weak mixing, and the operators we are using for the  $0^{-+}$  glueball have a strong overlap with the first excited state, but a very weak one with lowest state.

From figure 5 we can see moreover that the first excited state of the  $0^{++}$  glueball is compatible with the lightest state of the  $0^{-+}$  glueball. In combination with an additional excited gluino-gluon, this would be a multiplet of excited states. This line of reasoning seems to indicate that the glueball states have an energy higher than the gluinoball as argued in [28].

### 5.3 Comparison between $r_0$ and $w_0$

The lattice spacing has been defined in terms of  $w_0$  in the extrapolation to the continuum limit. For the interpretation of the results it is interesting to express them in units of the Sommer scale  $r_0$ , which is around 0.5 fm in QCD. There are two possible ways to get these results: on the one hand the dimensionless ratio  $r_0/w_0$  can be extrapolated to the continuum limit and used to convert the above continuum results to the scale  $r_0$ ; on the other hand the extrapolations to the continuum limit can alternatively be done using the value of  $a/r_0$  as implicit definition of the lattice spacing. The two different procedures can be used to test the systematic error of the extrapolation to the continuum limit. In fact, assuming that the asymptotic scaling region has already been reached, the two procedures

must give compatible results. If not, this would be a signal of the fact that the extrapolation to the continuum limit is not yet stable.

Using  $r_0$  as scale parameter to extrapolate to the continuum limit we get the results labelled as  $s = r_0$  in table 4. The dimensionless ratio  $r_0/w_0$  extrapolated to the continuum limit is

$$r_0/w_0 = 2.21(12). \tag{5.5}$$

Using this value to convert the masses, which have been extrapolated to the continuum limit using  $r_0$ , in terms of  $w_0$  we get the values labelled with  $w_0^*$  in table 4. We note that for  $\beta = 1.6$  we have recalculated the Sommer parameter  $r_0$  in order to apply a uniform methodology for all values of  $\beta$ . The results for  $r_0$  are slightly different from the old ones in [8], since by a refined choice of fit ranges we could obtain more reliable results.

For all particles, the masses determined with these two procedures are compatible within 1.4 standard deviations. However, the use of  $r_0$  results in a slightly larger mass gap between the gluino-gluon and the  $a-\eta'$  masses. Other possible choices to set the scale, like  $t_0$  or  $w_0$  at a different reference value, give an almost perfect compatibility, related to the fact that they do not refer to completely independent observable.

## 6 Improved lattice formulations

In the continuum extrapolation we have found a particle spectrum compatible with the formation of a supermultiplet and unbroken supersymmetry. This is also compatible with theoretical considerations that have found a non-zero Witten index of the theory. We can now invert the argument and take the separation of the multiplets as a signal for the lattice artefacts of the chosen discretisation. Consequently, the best choice for further investigations of the theory on the lattice is the discretisation with the smallest separation of the particles in the multiplet.

At  $\beta = 1.75$  we have done a reasonable amount of simulations with three, instead of one, level of stout smearing. We have found that the fluctuations of the lowest eigenvalues of the Hermitian Wilson-Dirac operator are considerably reduced with the additional levels of stout smearing, but the results for the mass spectrum are consistent with the data from one level of smearing. Hence this modification represents rather a technical improvement than a reduction of the lattice artefacts.

Symanzik's improvement program [29, 30] provides a systematic way to cancel the leading  $O(a)$  lattice artefacts of the Curci-Veneziano action. The fermion action is modified by the addition of an irrelevant operator, the so-called clover term,

$$- c_{sw} \frac{a}{4} \bar{\lambda}(x) \sigma_{\mu\nu} F^{\mu\nu} \lambda(x). \tag{6.1}$$

The coefficient  $c_{sw}$  is tuned such that  $O(a)$  lattice artefacts are removed from on-shell quantities, like for instance masses of physical particles [31–33]. The perturbative calculation of  $c_{sw}$  has been presented up to  $O(g^2)$  for  $\mathcal{N} = 1$  SYM in ref. [34]. It is, however, well known that higher order corrections to  $c_{sw}$  are non-negligible in the range of gauge couplings used in practical Monte Carlo simulations [34, 35].

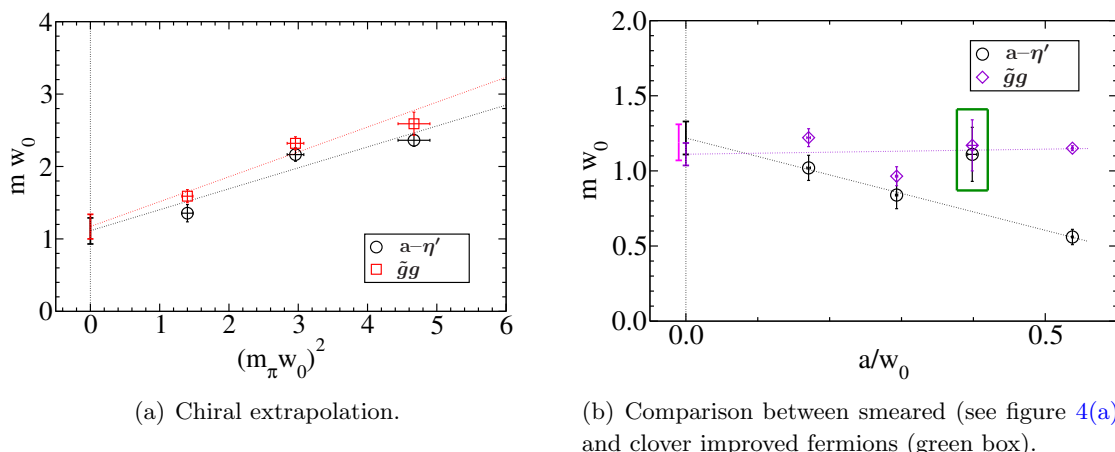


**Figure 6.** (a) Extrapolation of the  $a\text{-}\eta'$  and gluino-gluon ( $\tilde{g}g$ ) masses to the chiral limit computed with tadpole improved clover fermions. (b) Comparison of the extrapolations to the continuum limit of the  $a\text{-}\eta'$  and gluino-gluon masses with the tadpole clover improved action results (green box).

An alternative to the perturbative result is given by a mean-field rescaling of the link variables with the fourth root of the plaquette,  $u_0 = \langle P \rangle^{1/4}$ , due to a suppression of tadpole diagrams [36]. The resulting clover coefficient reads

$$c_{sw} = \frac{1}{u_0^3}. \tag{6.2}$$

We have done some preliminary simulations of tadpole improved clover fermions without stout smearing. The results are summarised in table 2. The chiral extrapolated value of  $w_0$  is determined to be  $w_0 = 2.51(4)$ . We measured the plaquette expectation value at  $\beta = 1.7$  extrapolated to the chiral limit and, using the formula above, we set  $c_{sw} = 1.467$ . The limited statistics allows only for a determination of the  $a\text{-}\eta'$  and gluino-gluon mass. The chiral extrapolation is presented in figure 6(a). It is interesting to observe that despite the large lattice spacing, the values of the masses extrapolated to the chiral limit are already compatible with their values extrapolated to the continuum limit using the one-level stout smeared action, see figure 6(b).

## 7 Conclusions

In this paper we have presented our latest results on the spectrum of bound states in SYM. Reliable lattice simulations are now possible thanks to the evolution of supercomputers and algorithms in recent years. Another important step has been the localisation of the reliable parameters range for the simulations which is limited by finite size effects and topological freezing.

Based on these recent developments we have generated a large set of configurations at different lattice spacings and gluino masses over several years. At each lattice spacing we have performed an extrapolation of the lowest bound state masses in the scalar, pseudoscalar, and spin-1/2 channel to the chiral limit at zero gluino mass. As we have shown,

this limit is compatible with the restoration of the supersymmetric Ward identities. Our last set of data at  $\beta = 1.9$  allows to complete the extrapolation to the continuum limit.

The extrapolations to the continuum limit show agreement for the masses within less than two standard deviations. This is consistent with the formation of a SUSY multiplet, which is expected to contain a scalar and a pseudoscalar boson in addition to the fermion.

There are two important conclusions that can be drawn from these observations: a proper non-perturbative definition of the strongly interacting supersymmetric theory is possible and there is no breaking of SUSY in the low energy effective theory. This is equivalent to the absence of an anomalous or spontaneous SUSY breaking in this theory.

Taking the unbroken SUSY in the continuum theory for granted, the second conclusion is that the lattice method can be applied in a non-trivial four-dimensional supersymmetric theory. SUSY, which is unavoidably broken by the discretisation, is like Lorentz symmetry and chiral symmetry restored in the continuum limit in SYM. In our case, this is achieved by a fine-tuning of the hopping parameter.

In a first, short study we have shown that the breaking of SUSY indicated by the mass splitting of the multiplet on a coarse lattice is significantly reduced when a tadpole improved clover fermion action is used. In addition, technical aspects of the methods are improved by stout smearing in the Dirac operator. This indicates that clover improved fermions with stout smearing seem to be the best choice for future lattice investigations of the theory.

In our present investigation we considered only the mass of the lightest supermultiplet. A second chiral supermultiplet with higher mass has been predicted [3, 4, 28]. The determination of the mass of the second supermultiplet on the lattice requires the computation of the mixing between gluonic and fermionic operators. We plan to investigate this aspect in the near future. The analysis of the mass of the pseudoscalar glueball and of the excited state of the scalar glueball indicates that mixing might be rather weak in the  $0^{-+}$  channel. In this case, the second excited supermultiplet appears to be roughly twice as massive as the ground state.

## Acknowledgments

The authors gratefully acknowledge the Gauss Centre for Supercomputing (GCS) for providing computing time for a GCS Large-Scale Project on the GCS share of the supercomputer JUQUEEN at Jülich Supercomputing Centre (JSC). GCS is the alliance of the three national supercomputing centres HLRS (Universität Stuttgart), JSC (Forschungszentrum Jülich), and LRZ (Bayerische Akademie der Wissenschaften), funded by the German Federal Ministry of Education and Research (BMBF) and the German State Ministries for Research of Baden-Württemberg (MWK), Bayern (StMWFK) and Nordrhein-Westfalen (MIWF). Further computing time has been provided on the supercomputers JURECA and JUROPA at JSC, SuperMUC at LRZ, and on the compute cluster PALMA of the University of Münster.

## A Tables

$\kappa$	# confs	$am_{a-\pi}$	$am_{a-\eta'}$	$am_{a-f_0}$	$am_{\tilde{g}g}$	$m_{gb}(0^{++})$	$m_{gb}(0^{-+})$
0.1433	10374	0.28737(84)	0.314(18)	0.313(84)	0.324(11)	0.35(2)	0.60(3)
0.14387	10237	0.21410(33)	0.260(11)	0.265(53)	0.295(10)	0.27(3)	0.52(6)
0.14415	21090	0.17520(22)	0.232(11)	0.262(25)	0.236(15)	0.29(2)	0.52(4)
0.14435	10680	0.14129(59)	0.203(12)	0.227(19)	0.2360(74)	0.29(3)	0.52(3)

**Table 1.** Summary of the masses in lattice units for the one-level stout smeared action at  $\beta = 1.9$ , lattice size  $32^3 \times 64$ .

$\kappa$	# configs	$w_0/a$	$am_{a-\pi}$	$am_{a-\eta'}$	$am_{\tilde{g}g}$
0.1600	4043	1.7456(87)	0.8606(71)	0.941(18)	1.030(46)
0.1620	3474	1.915(11)	0.6851(28)	0.862(23)	0.924(20)
0.1640	1466	2.165(15)	0.4716(54)	0.540(39)	0.633(26)

**Table 2.** Summary of the masses in lattice units for the tadpole clover improved action at  $\beta = 1.7$ ,  $c_{sw} = 1.467$ , lattice size  $16^3 \times 32$ .

$\beta$	$am_{a-\eta'}$	$am_{a-f_0}$	$am_{\tilde{g}g}$	$am_{gb}(0^{++})$	$am_{gb}(0^{-+})$	$w_0/a$	$r_0/a$
1.90	0.174(14)	0.201(35)	0.208(10)	0.253(26)	0.486(35)	5.858(84)	13.95(12)
$1.75^{l=1}$	0.246(26)	0.228(71)	0.283(18)	0.294(62)	0.63(22)	3.411(18)	9.47(14)
$1.75^{l=3}$	0.268(22)	0.331(30)	0.3295(83)	0.393(33)	1.014(20)	3.189(11)	9.28(7)
1.60	0.301(27)	0.256(81)	0.619(86)	0.51(13)	—	1.8595(39)	5.78(15)

**Table 3.** Summary of the masses and scale parameters in lattice units extrapolated to the chiral limit ( $\kappa = \kappa_c$ ). For  $\beta = 1.75$  we report the values for one ( $l = 1$ ) and three ( $l = 3$ ) levels of stout smearing.

	$sm_{a-\eta'}$	$sm_{a-f_0}$	$sm_{\tilde{g}g}$	$sm_{gb}(0^{++})$
$s = r_0$	2.97(33)	3.67(85)	2.23(23)	3.96(83)
$s = w_0$	1.22(11)	1.43(28)	1.111(74)	1.67(25)
$s = w_0^* = r_0/(r_0/w_0)$	1.34(17)	1.66(40)	1.01(12)	1.79(39)
$(w_0^* - w_0)/\Delta w_0$	1.09	0.82	1.36	0.48

**Table 4.** Summary of the masses extrapolated to the continuum limit using different scales.  $w_0^*$  is a parameter determined from  $r_0$  using the ratio  $r_0/w_0 = 2.21(12)$ . In the last row the comparison between  $w_0$  and  $w_0^*$  is shown. In this table the mass of the glueball  $0^{-+}$  is not present because we have not enough data for the extrapolation to the continuum limit.

**Open Access.** This article is distributed under the terms of the Creative Commons Attribution License ([CC-BY 4.0](https://creativecommons.org/licenses/by/4.0/)), which permits any use, distribution and reproduction in any medium, provided the original author(s) and source are credited.

## References

- [1] D. Amati, K. Konishi, Y. Meurice, G.C. Rossi and G. Veneziano, *Nonperturbative aspects in supersymmetric gauge theories*, *Phys. Rept.* **162** (1988) 169 [[INSPIRE](#)].
- [2] G. Veneziano and S. Yankielowicz, *An effective lagrangian for the pure  $N = 1$  supersymmetric Yang-Mills theory*, *Phys. Lett. B* **113** (1982) 231 [[INSPIRE](#)].
- [3] G.R. Farrar, G. Gabadadze and M. Schwetz, *On the effective action of  $N = 1$  supersymmetric Yang-Mills theory*, *Phys. Rev. D* **58** (1998) 015009 [[hep-th/9711166](#)] [[INSPIRE](#)].
- [4] G.R. Farrar, G. Gabadadze and M. Schwetz, *The spectrum of softly broken  $N = 1$  supersymmetric Yang-Mills theory*, *Phys. Rev. D* **60** (1999) 035002 [[hep-th/9806204](#)] [[INSPIRE](#)].
- [5] L. Bergamin and P. Minkowski, *SUSY glue balls, dynamical symmetry breaking and nonholomorphic potentials*, [hep-th/0301155](#) [[INSPIRE](#)].
- [6] C. McNeile, *Lattice status of gluonia/glueballs*, *Nucl. Phys. Proc. Suppl.* **186** (2009) 264 [[arXiv:0809.2561](#)] [[INSPIRE](#)].
- [7] G. Bergner, *Complete supersymmetry on the lattice and a No-Go theorem*, *JHEP* **01** (2010) 024 [[arXiv:0909.4791](#)] [[INSPIRE](#)].
- [8] K. Demmouche et al., *Simulation of 4D  $N = 1$  supersymmetric Yang-Mills theory with Symanzik improved gauge action and stout smearing*, *Eur. Phys. J. C* **69** (2010) 147 [[arXiv:1003.2073](#)] [[INSPIRE](#)].
- [9] G. Bergner, G. Münster, D. Sandbrink, U.D. Özugurel and I. Montvay, *Supersymmetric Yang-Mills theory: a step towards the continuum*, [arXiv:1111.3012](#) [[INSPIRE](#)].
- [10] G. Bergner et al., *The gluino-gluon particle and finite size effects in supersymmetric Yang-Mills theory*, *JHEP* **09** (2012) 108 [[arXiv:1206.2341](#)] [[INSPIRE](#)].
- [11] G. Bergner, I. Montvay, G. Münster, D. Sandbrink and U.D. Ozugurel, *The gluino-gluon particle and relevant scales for the simulations of supersymmetric Yang-Mills theory*, *PoS(LATTICE 2012)042* [[arXiv:1210.7767](#)] [[INSPIRE](#)].
- [12] G. Bergner, I. Montvay, G. Münster, U.D. Özugurel and D. Sandbrink, *Towards the spectrum of low-lying particles in supersymmetric Yang-Mills theory*, *JHEP* **11** (2013) 061 [[arXiv:1304.2168](#)] [[INSPIRE](#)].
- [13] G. Bergner, P. Giudice, G. Münster, S. Piemonte and D. Sandbrink, *Phase structure of the  $\mathcal{N} = 1$  supersymmetric Yang-Mills theory at finite temperature*, *JHEP* **11** (2014) 049 [[arXiv:1405.3180](#)] [[INSPIRE](#)].
- [14] G. Curci and G. Veneziano, *Supersymmetry and the lattice: a reconciliation?*, *Nucl. Phys. B* **292** (1987) 555 [[INSPIRE](#)].
- [15] C. Morningstar and M.J. Peardon, *Analytic smearing of SU(3) link variables in lattice QCD*, *Phys. Rev. D* **69** (2004) 054501 [[hep-lat/0311018](#)] [[INSPIRE](#)].
- [16] H. Suzuki, *Supersymmetry, chiral symmetry and the generalized BRS transformation in lattice formulations of 4D  $\mathcal{N} = 1$  SYM*, *Nucl. Phys. B* **861** (2012) 290 [[arXiv:1202.2598](#)] [[INSPIRE](#)].
- [17] G. Münster and H. Stüwe, *The mass of the adjoint pion in  $\mathcal{N} = 1$  supersymmetric Yang-Mills theory*, *JHEP* **05** (2014) 034 [[arXiv:1402.6616](#)] [[INSPIRE](#)].



- [18] I. Montvay and E. Scholz, *Updating algorithms with multi-step stochastic correction*, *Phys. Lett. B* **623** (2005) 73 [[hep-lat/0506006](#)] [[INSPIRE](#)].
- [19] G. Bergner and J. Wuilloud, *Acceleration of the Arnoldi method and real eigenvalues of the non-Hermitian Wilson-Dirac operator*, *Comput. Phys. Commun.* **183** (2012) 299 [[arXiv:1104.1363](#)] [[INSPIRE](#)].
- [20] J. Giedt, R. Brower, S. Catterall, G.T. Fleming and P. Vranas, *Lattice super-Yang-Mills using domain wall fermions in the chiral limit*, *Phys. Rev. D* **79** (2009) 025015 [[arXiv:0810.5746](#)] [[INSPIRE](#)].
- [21] M.G. Endres, *Dynamical simulation of  $N = 1$  supersymmetric Yang-Mills theory with domain wall fermions*, *Phys. Rev. D* **79** (2009) 094503 [[arXiv:0902.4267](#)] [[INSPIRE](#)].
- [22] JLQCD collaboration, S.W. Kim et al., *Lattice study of 4d  $\mathcal{N} = 1$  super Yang-Mills theory with dynamical overlap gluino*, *PoS(LATTICE 2011)069* [[arXiv:1111.2180](#)] [[INSPIRE](#)].
- [23] M. Lüscher and S. Schaefer, *Lattice QCD without topology barriers*, *JHEP* **07** (2011) 036 [[arXiv:1105.4749](#)] [[INSPIRE](#)].
- [24] K. Demmouche,  *$\mathcal{N} = 1$  SU(2) supersymmetric Yang-Mills theory on the lattice with light dynamical Wilson gluinos*, Ph.D. thesis, University of Münster, Münster, Germany (2009).
- [25] APE collaboration, M. Albanese et al., *Glueball masses and string tension in lattice QCD*, *Phys. Lett. B* **192** (1987) 163 [[INSPIRE](#)].
- [26] DESY-MUNSTER-ROMA collaboration, F. Farchioni et al., *The supersymmetric Ward identities on the lattice*, *Eur. Phys. J. C* **23** (2002) 719 [[hep-lat/0111008](#)] [[INSPIRE](#)].
- [27] G. Bergner, P. Giudice, I. Montvay, G. Münster and S. Piemonte, *Influence of topology on the scale setting*, *Eur. Phys. J. Plus* **130** (2015) 229 [[arXiv:1411.6995](#)] [[INSPIRE](#)].
- [28] A. Feo, P. Merlatti and F. Sannino, *Information on the super Yang-Mills spectrum*, *Phys. Rev. D* **70** (2004) 096004 [[hep-th/0408214](#)] [[INSPIRE](#)].
- [29] K. Symanzik, *Continuum limit and improved action in lattice theories. 1. Principles and  $\phi^4$  theory*, *Nucl. Phys. B* **226** (1983) 187 [[INSPIRE](#)].
- [30] K. Symanzik, *Continuum limit and improved action in lattice theories. 2.  $O(N)$  nonlinear  $\sigma$ -model in perturbation theory*, *Nucl. Phys. B* **226** (1983) 205 [[INSPIRE](#)].
- [31] M. Lüscher and P. Weisz, *On-shell improved lattice gauge theories*, *Commun. Math. Phys.* **97** (1985) 59 [*Erratum ibid.* **98** (1985) 433] [[INSPIRE](#)].
- [32] B. Sheikholeslami and R. Wohlert, *Improved continuum limit lattice action for QCD with Wilson fermions*, *Nucl. Phys. B* **259** (1985) 572 [[INSPIRE](#)].
- [33] R. Wohlert, *Improved continuum limit lattice action for quarks*, report DESY-87-069 (1987).
- [34] S. Musberg, G. Münster and S. Piemonte, *Perturbative calculation of the clover term for Wilson fermions in any representation of the gauge group SU(N)*, *JHEP* **05** (2013) 143 [[arXiv:1304.5741](#)] [[INSPIRE](#)].
- [35] T. Karavirta, K. Tuominen, A. Mykkanen, J. Rantaharju and K. Rummukainen, *Non-perturbatively improved clover action for SU(2) gauge + fundamental and adjoint representation fermions*, *PoS(LATTICE 2010)064* [[arXiv:1011.1781](#)] [[INSPIRE](#)].
- [36] G.P. Lepage and P.B. Mackenzie, *On the viability of lattice perturbation theory*, *Phys. Rev. D* **48** (1993) 2250 [[hep-lat/9209022](#)] [[INSPIRE](#)].